

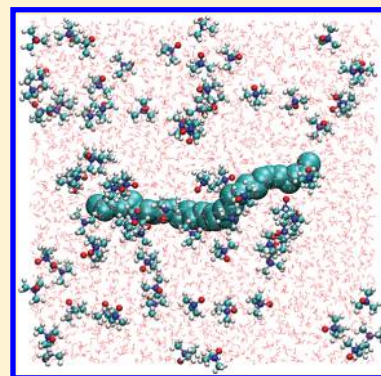
# When Does Trimethylamine *N*-Oxide Fold a Polymer Chain and Urea Unfold It?

Jagannath Mondal, Guillaume Stirnemann, and B. J. Berne\*

Department of Chemistry, Columbia University, 3000 Broadway, New York, New York 10027, United States

## S Supporting Information

**ABSTRACT:** Longstanding mechanistic questions about the role of protecting osmolyte trimethylamine *N*-oxide (TMAO) that favors protein folding and the denaturing osmolyte urea are addressed by studying their effects on the folding of uncharged polymer chains. Using atomistic molecular dynamics simulations, we show that 1 M TMAO and 7 M urea solutions act dramatically differently on these model polymer chains. Their behaviors are sensitive to the strength of the attractive dispersion interactions of the chain with its environment: when these dispersion interactions are sufficiently strong, TMAO suppresses the formation of extended conformations of the hydrophobic polymer as compared to water while urea promotes the formation of extended conformations. Similar trends are observed experimentally for real protein systems. Quite surprisingly, we find that both protecting and denaturing osmolytes strongly interact with the polymer, seemingly in contrast with existing explanations of the osmolyte effect on proteins. We show that what really matters for a protective osmolyte is its effective depletion as the polymer conformation changes, which leads to a negative change in the preferential binding coefficient. For TMAO, there is a much more favorable free energy of insertion of a single osmolyte near collapsed conformations of the polymer than near extended conformations. By contrast, urea is preferentially stabilized next to the extended conformation and thus has a denaturing effect.



## I. INTRODUCTION

Osmolytes are small cosolutes found endogenously to protect cells against osmotic stress.<sup>1</sup> However, they can have profound effects on protein stability.<sup>2–8</sup> While some of them are denaturants (e.g., urea), others like trimethylamine *N*-oxide (TMAO) act as protecting osmolytes *in vivo*: under denaturing conditions, they bias the protein structure toward the folded conformation.<sup>1,9–12</sup> They are thus termed chemical chaperones. Hence, TMAO is used by deep-sea organisms to counteract the deleterious effect of pressure and by sharks or skates to compensate for their relatively high concentrations of denaturing urea.<sup>11</sup> Most interestingly, the protein folding propensity of TMAO has been used experimentally to study the mechanisms involved in protein misfolding diseases, including, e.g., prion protein,<sup>13,14</sup> tau protein<sup>15,16</sup> (Alzheimer's disease), and  $\alpha$ -synuclein<sup>17</sup> (involved in numerous neurodegenerative diseases); chemical chaperones like TMAO even appear to be promising as therapeutics,<sup>18</sup> even though it was recently found to be related to an increased risk of cardiovascular diseases in humans.<sup>19</sup> TMAO is active in endogenous systems at concentrations as low as 200 mM.<sup>1,13</sup> Experiments *in vitro* with  $\alpha$ -synuclein, an intrinsically disordered protein, have provided evidence that the strength of this protective effect increases with concentration.<sup>17</sup>

TMAO is a small amphiphile [chemical formula,  $(\text{CH}_3)_3\text{NO}$ ] consisting of a small hydrophilic group ( $\text{N}^+\text{O}^-$ ) and a bulky hydrophobic part (three methyl groups). Several mechanisms have been invoked to explain the folding propensity of TMAO.

In the first scenario, TMAO would enhance water structure and hydrogen bond (HB) strength, which would indirectly affect the equilibrium between the folded and unfolded conformations of a protein.<sup>20–22</sup> However, this mechanism has been challenged by several studies, mainly based on molecular dynamics (MD) simulations, in which no significant alteration of water structure was found in aqueous solutions of TMAO.<sup>23–25</sup> These results may not be surprising because TMAO can accept only two or three strong HBs at its hydrophilic head, which represents less than 10% of its hydration water HB population.<sup>26</sup>

Other studies have suggested that direct interactions, or especially the lack thereof, between TMAO and the protein backbone could cause the osmolyte effect. In particular, thermodynamic measurements have highlighted the importance of the interactions between TMAO and the protein backbone and side chains.<sup>9,10</sup> TMAO has favorable interactions with some protein side chains, especially the positively charged groups that can interact with the  $\text{O}^-$  of TMAO. In contrast, interactions with the protein backbone, in particular with the amide NH, are entropically unfavorable.<sup>24</sup> If these unfavorable interactions were to dominate, TMAO would be depleted from the protein surface. It has been suggested that the resulting concentration gradient in the TMAO could lead to an osmotic pressure

Received: June 6, 2013

Revised: June 25, 2013

Published: June 25, 2013

favoring the folded conformation with respect to the unfolded one.<sup>24</sup> Recently, Garcia and co-workers have combined<sup>27</sup> computer simulation with the experimental osmotic pressure measurements and have suggested a mechanism in which there is preferential exclusion of TMAO from protein surfaces because of repulsive self-interaction in the solvation shell. Others have argued that osmotic pressure itself cannot explain this phenomenon, and that “water-mediated interactions” between the osmolyte and the protein could also play a role.<sup>25</sup>

However, a clear unifying scenario has not yet emerged from the study of the effect of TMAO on proteins. One of the reasons might be the presence of amino acids with different chemical properties that might complicate the role of TMAO as a structure enhancer. Thus, instead of struggling with different amino acids, a successful strategy can be to use a simple polymeric chain whose hydrophobicity can be tuned. There have already been studies of the action of TMAO on purely hydrophobic chains,<sup>23</sup> but even for such a simple system, a consensus has not yet been achieved. A good illustration of the lack of consensus is the opposite conclusions reached in two different investigations. On the basis of simulations of small hydrophobic solutes and hydrophobic chains, one of these studies suggested that TMAO has a negligible effect on the hydrophobic interactions.<sup>23</sup> In contrast, other studies suggest that TMAO destroys hydrophobic interactions.<sup>28</sup>

To investigate the molecular mechanism of TMAO's role as a protective osmolyte, it is interesting to compare it with the effect of urea [chemical formula,  $(\text{NH}_2)_2\text{CO}$ ] solutions that leads to the opposite behavior, unfolding of the protein. For example, Pettitt and co-workers<sup>29</sup> have recently explored the conformational preferences of decaalanine in TMAO and urea solutions using free energy perturbation techniques. Their analysis, based on the decomposition of the transfer free energy, suggests the differences in the behavior of peptide in the two different solutions arise mainly from differences in the relative importance of van der Waals and electrostatic interactions: urea denaturation is dominated by van der Waals attractions, whereas TMAO exerts its effect by causing unfavorable electrostatic interactions. In this work, we extend our previous work on urea<sup>30</sup> by using similar systems and methodologies and apply it to contrast the respective role of a denaturing osmolyte (urea) and a protective osmolyte (TMAO) on uncharged chains in water. We focus on the mechanisms by which these two osmolytes produce opposite actions on the conformations of this Lennard-Jones chain. Following most of the previous simulation studies, we used concentrations higher than that found *in vivo* to enhance the influence of the osmolyte on protein stability. Hence, we chose a concentration of 7 M for urea (consistent with ref 30) and a concentration of 1 M for TMAO. Both concentrations are widely used to study the effects of the respective osmolytes *in vitro* and *in silico*. Our study shows that while acting on the same chain, TMAO stabilizes the collapsed conformations of the chain while urea destabilizes the collapsed conformations, and the simulations later allow us to offer a molecular explanation for these different behaviors. The paper is organized as follows: The simulation model and methods are described in section II. Results are presented in section III. Some conclusions are presented in section IV.

## II. SIMULATION MODEL AND METHODS

**System and Force Fields.** Our system consists of a 32-bead polymer solvated in various aqueous solutions. The

polymer is uncharged, and the beads interact with their environment only via Lennard-Jones (LJ) potentials. While the bead radius is fixed ( $\sigma_b = 0.4$  nm), the hydrophobic character of the chain can be tuned by varying the energy parameter  $\epsilon_b$ . Following a previous study,<sup>30</sup> four values were employed ( $\epsilon_b = 0.4, 0.6, 0.8,$  and  $1.0$  kJ/mol) even if most of the current work was performed on the  $\epsilon_b = 1.0$  kJ/mol polymer. Among the chain, 1–4 interactions were removed; parameters for the 1–2 (bonds) and 1–3 (angles) interactions can be found elsewhere.<sup>30</sup> For water molecules, we used the SPC/E model,<sup>31</sup> while urea interacts through the OPLS/AA force field<sup>32</sup> and TMAO through the force field developed by Kast et al.<sup>33</sup> The geometric combining rules were used in the cross interactions for  $\epsilon$ , and arithmetic combination rules were used for  $\sigma$ . Three systems were simulated. The system of a pure aqueous solution was composed of the polymer solvated by 4092 water molecules. The system of the 1 M TMAO solution was composed of the 32-bead polymeric chain, 79 TMAO molecules, and 4013 water molecules. On the other hand, the system of the 7 M urea solution was composed of the 32-bead polymeric chain, 500 urea molecules, and 2727 water molecules. The box size was close to  $5 \text{ nm} \times 5 \text{ nm} \times 5 \text{ nm}$  in all cases. We have also repeated our simulation for TMAO at an  $\epsilon_b$  of 1.0 kJ/mol using a different force field (called herein the “osmotic model”) recently proposed by Garcia and co-workers,<sup>27</sup> and we found it to follow the same qualitative trends (cf. the text of the Supporting Information).

**Equilibrium Simulations.** All simulations were performed using Gromacs version 4.5.4.<sup>34</sup> In a bid to sample different polymer conformations in different osmolyte solutions, unrestrained equilibrium MD simulations of the polymer chain were performed in pure water and in 1 M TMAO and 7 M urea solutions. To avoid any bias, an extended configuration of the polymeric chain was used as an initial configuration in pure water and in the aqueous solution of 1 M TMAO while a collapsed configuration of the polymer was used as an initial configuration for the simulation in the aqueous solution of 7 M urea. The initial extended configuration was an all-*trans* configuration of the polymer, while the collapsed configuration was picked from the simulation of the polymer in water. Each of the systems was first energy-minimized using a steepest-descent algorithm and then subjected to a 100 ns production run in the *NPT* ensemble. The Nose-Hoover thermostat was used for maintaining the average temperature of 300 K, and the Parinello-Rahman barostat was used for maintaining the average pressure of 1 bar. For all three aqueous solutions, unrestrained simulations were repeated for the four values of the LJ energy parameter ( $\epsilon_b$ ) for the polymer beads.

**Potentials of Mean Force.** We determined the free energy landscape [or potential of mean force (PMF)] of the 32-bead LJ chains along one or several collective reaction coordinates in different solutions by performing umbrella sampling simulations. We chose as a reaction coordinate the polymer radius of gyration ( $R_g$ ) in pure water, 1 M TMAO, and 7 M urea. We employed the PLUMED extension of Gromacs.<sup>35</sup> The value of  $R_g$  ranged from 0.4 to 1.2 nm at a spacing of 0.05 nm between adjacent windows. Restraining harmonic force constants of  $7000 \text{ kJ mol}^{-1} \text{ nm}^{-2}$  were used in the umbrella potential in all positions to ensure a Gaussian distribution of the reaction coordinate around each desired value of the reaction coordinate. Finally, we used the weighted histogram analysis method (WHAM)<sup>36,37</sup> to generate unbiased histograms and corresponding free energies. As described later, we also

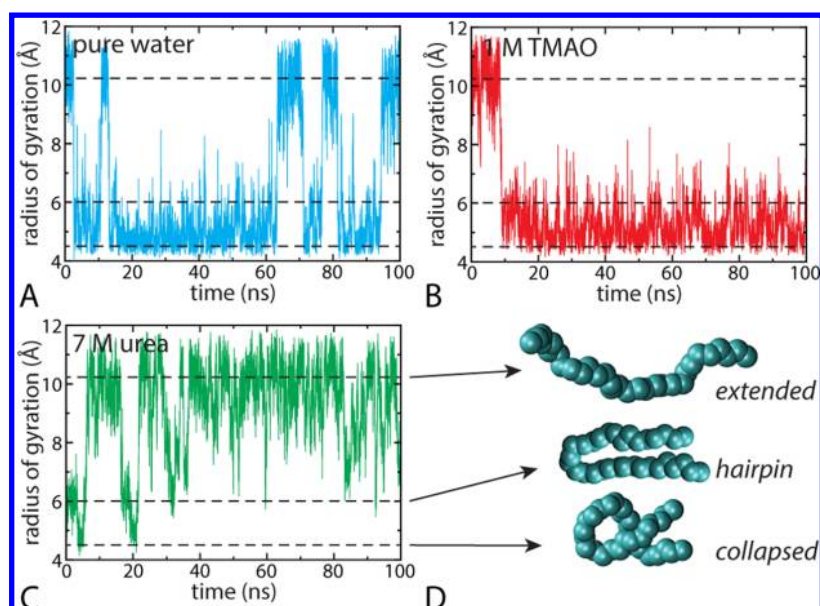


**Figure 1.** Time profile of the polymer's radius of gyration for an  $\epsilon_b$  of 1.0 kJ/mol as obtained from unrestrained simulations in different aqueous solutions: (A) water, (B) 1 M TMAO solution, and (C) 7 M urea solution. The horizontal dashed lines corresponding to  $R_g$  values of 4.5, 6.0, and 10.2 Å represent the most probable values of the radius of gyration for the collapsed (folded), hairpinlike, and extended (unfolded) conformations, respectively, depicted in panel D.

compute the joint probability distribution of  $R_g$  and the end-to-end distance and the corresponding potential of mean force as a function of these two variables.

**Preferential Interaction.** We employed two parameters to measure the affinity of the cosolvent (urea or TMAO) for the polymer. First, the local bulk partition coefficient ( $K_p$ ) was calculated, as<sup>7</sup>

$$K_p = \frac{\langle n_s \rangle N_w^{\text{tot}}}{\langle n_w \rangle N_s^{\text{tot}}} \quad (1)$$

where  $\langle n_x \rangle$  is the average number of molecules of type X bound to the polymer and  $N_x^{\text{tot}}$  is the total number of molecules of type X in the system [where X = s stands for the cosolvent (urea or TMAO) and X = w stands for water].  $K_p$  is intensive and reflects the affinity of the cosolvent for the polymer regardless of the exposed surface area of the polymer. The other parameter is the experimentally relevant preferential binding coefficient<sup>2,3,7,27,38</sup>

$$\Gamma = \left\langle n_s - \frac{N_s^{\text{tot}} - n_s}{N_w^{\text{tot}} - n_w} \times n_w \right\rangle \quad (2)$$

which is extensive (i.e., it depends on the size of the hydration shell). To determine the dependence on the proximal cutoff distance for the counting of molecules around the polymer, we computed the value of both quantities  $K_p$  and  $\Gamma$  as a function of distance from the polymer [i.e., by examining the explicit distance dependence of  $n_s(r)$  and  $n_w(r)$ ], which is defined as the shortest distance between the central atom of the solvent molecule (O for water, N for TMAO, and C for urea) and any polymer bead. Additional simulations were performed as follows. We froze five representative configurations of the polymer in either the collapsed or the extended state for each osmolyte solution and then propagated each of these simulations for 15 ns (total simulation length of 75 ns for each polymer configuration). In each case, both  $K_p$  and  $\Gamma$  were

averaged over this ensemble of trajectories, and standard deviations were obtained via block averaging.

Finally, we used the free energy perturbation (FEP) technique to compute the transfer free energy (chemical potential) for inserting a single TMAO (or urea or water molecule) from bulk solution into the first solvation shell of particular conformations of the polymer in 1 M TMAO (or 7 M urea) where the polymer conformation was fixed in either a collapsed or an extended conformation. For these calculations, the initial configurations were taken from a representative snapshot of the prior umbrella sampling windows and the TMAO (or urea or water) molecule was grown in presence of other TMAO (or urea or water) molecules in solution. The interactions of the molecule being inserted were slowly turned on in two stages: in the first stage, only the van der Waals interactions were turned on, and in the second stage, the electrostatic interactions were turned on. Thermodynamic integration gives these two contributions to the transfer free energy. The difference between the free energy for the insertion proximate to the polymer and the insertion in bulk gives the required transfer free energies. Finally, because the choice of the position near the polymer where the osmolyte and solvent molecules is grown is arbitrary, we repeated such calculations at several positions in each case: five sites for TMAO and urea and three sites for water near each of the collapsed and extended conformations and two sites of each of them in bulk media. They were finally averaged, and the standard deviations were estimated.

### III. RESULTS AND DISCUSSION

**Osmolyte Effect on Folding Equilibria.** We first verify that the effects of TMAO and urea on an uncharged Lennard-Jones polymer chain are those observed in protein systems, i.e., that they act as protective and denaturing osmolytes, respectively. Toward this end, a reasonable approach is to follow the time evolution of an order parameter describing the polymer conformation, like its radius of gyration that will allow

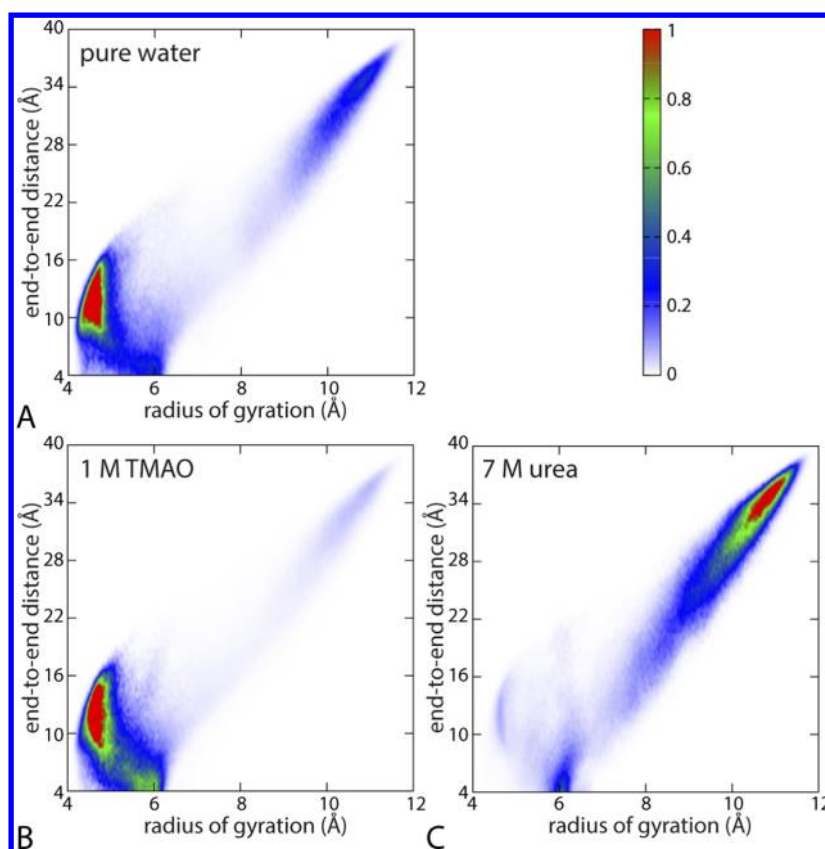


**Figure 2.** Comparison of the joint probability distribution of the polymer chain ( $\epsilon_b = 1$  kJ/mol) along the radius of gyration and end-to-end distance (A) in water, (B) in 1 M TMAO, and (C) in 7 M urea, obtained from umbrella sampling simulations.

us to distinguish between the collapsed and extended configurations. Such profiles are shown for a polymer with a bead interaction parameter  $\epsilon_b$  of 1.0 kJ/mol in Figure 1. For these unrestrained simulations, the initial configurations in each system (water, 1 M TMAO, and 7 M urea) were chosen anticipating the effect of this aqueous solution on the polymer conformational equilibrium. Thus, simulations were started from an unfolded state in water and TMAO solutions ( $R_g = 11.5$  Å) and from a collapsed configuration ( $R_g = 4.5$  Å) in the urea solution. Each of these simulations was then propagated for 100 ns.

Figure 1 shows that the polymeric chain behaves very differently in the three environments. In water (Figure 1A), the initially extended polymer quickly collapses and then fluctuates between the collapsed and extended configurations. In the TMAO solution (Figure 1B), the polymer collapses and remains compact for the whole 100 ns time scale: the extended configuration sampled in pure water is not observed in TMAO on the time scale of the simulation. In contrast, the polymer in urea unfolds (Figure 1C) but very occasionally revisits more compact states like the hairpin at an  $R_g$  of  $\approx 0.6$  nm and very rarely visits the most compact states seen in water.

We thus see that for an  $\epsilon_b$  of 1.0 kJ/mol, TMAO and urea act as protective and denaturing osmolytes, respectively, with respect to the hydrophobic chain. This was already observed for urea,<sup>30</sup> albeit for a different water model (TIP4P<sup>39</sup>). It is remarkable that these osmolytes have similar effects on the hydrophobic chain and on real proteins. In the following, we aim to better understand this interesting behavior.

The semicompact hairpin configuration of the chain ( $R_g \approx 0.6$  nm) observed in the urea solution<sup>30</sup> (see Figure 1C) and to

some extent in water and the TMAO solution (panels A and B of Figure 1, respectively) can be better understood by considering a two-dimensional (2D) collective coordinate consisting of the radius of gyration and the end-to-end distance of the chain. Figure 2 shows joint probability  $P(L, R_g)$  of finding a polymer ( $\epsilon_b = 1.0$  kJ/mol) with end-to-end distance  $L$  and radius of gyration  $R_g$  for each of the systems shown in Figure 1. To avoid possible biases due to limited sampling in unperturbed simulations, the probability distribution of  $R_g$  is first recovered from the PMF obtained via umbrella sampling simulations. In each window, we later estimate conditional probability  $P(L|R_g)$  of finding  $L$  given  $R_g$ . The joint probability is finally recovered using the relation

$$P(L, R_g) = P(L|R_g) P(R_g) \quad (3)$$

The distributions shown in Figure 2 confirm our previous findings: in urea, the extended configurations are significantly more populated than in water, whereas in TMAO, they are essentially absent. Moreover, the hairpin state observed at an  $R_g$  of  $\approx 0.6$  nm and small  $L$  values in the 2D plots, although more prominent in the urea solution, also appear in the TMAO solution and in pure water. In contrast, the collapsed state around an  $R_g$  of  $\approx 0.45$  nm corresponds to a higher  $L$ , showing that the two order parameters are largely decoupled in this region of the distribution. Unfolded configurations correspond to high values of both  $L$  and  $R_g$  and give rise to distributions elongated along the diagonal in the 2D plots, and only urea has a strong peak there.

The potentials of mean force [ $W(R_g)$ ] as a function of the polymer radius of gyration ( $R_g$ ), obtained via umbrella sampling, and corresponding probability distributions

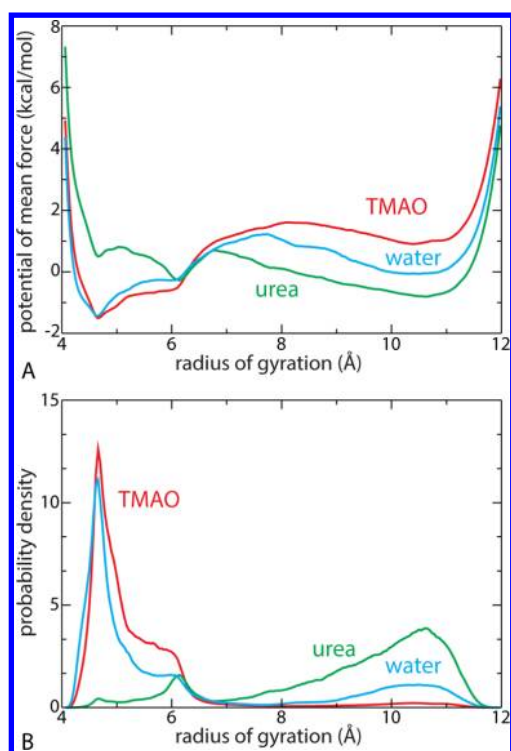


**Figure 3.** Potentials of mean force along the radius of gyration (A) and corresponding probability distributions (B) in the three aqueous solutions (water, blue; TMAO, red; urea, green) for polymer chains with an  $\epsilon_b$  of 1.0 kJ/mol. PMFs  $W(R_g)$  are normalized so that  $\int_0^\infty \exp[-W(r)/k_B T] dr = 1$ .

$\exp[-\beta W(R_g)]$  ( $\epsilon_b = 1.0$  kJ/mol) for the three aqueous solutions are shown in panels A and B of Figure 3, respectively (and in Figure S1 of the Supporting Information for other values of  $\epsilon_b$ ). These correspond to the projections of the joint probability distribution onto the radius of gyration axis. These provide a more reliable and quantitative description of the polymer conformational equilibrium than simulations based on unrestrained MD trajectories (Figure 1) because those would require much longer runs (as later illustrated by the free energy barriers of 2–4 kcal/mol between states).

As one can see in Figure 3, the unfolded state in the TMAO solution becomes destabilized with respect to pure water, whereas the collapsed state is not dramatically affected. Quite remarkably, the unfolded state is almost totally suppressed for TMAO, and its collapsed state is more compact for the  $\epsilon_b = 1.0$  kJ/mol case.

In previous molecular dynamics simulations of a similar system,<sup>23</sup> it was found that TMAO has little effect on the conformational equilibrium of a hydrophobic polymer chain. In that study, a lower polymer bead parameter ( $\epsilon_b$ ) of 0.6 kJ/mol was used versus that in our simulations. It is therefore important to determine the effect of the smaller  $\epsilon_b$  on the behavior of TMAO, as was done earlier for urea solutions.<sup>30</sup> In the text and Figure S1 of the Supporting Information, we show that as the hydrophobicity of the chain is increased or equivalently as  $\epsilon_b$  is decreased the chain responds differently to TMAO. The protecting effect of the 1 M TMAO solution is thus very sensitive to the value of  $\epsilon_b$ . We find that the protecting role of TMAO is very weak when the chain is strongly hydrophobic (low  $\epsilon_b$  values of 0.4 and 0.6 kJ/mol), in agreement with the conclusions of the previous study.<sup>23</sup>

However, TMAO's protecting role becomes much more prominent for larger  $\epsilon_b$  values of 0.8 and 1.0 kJ/mol.

As previously suggested using a different water model,<sup>30</sup> the response of the polymer to urea with a decrease in  $\epsilon_b$  is radically different. The trend is clearly opposite to that found in water or in the TMAO solution: the unfolded state becomes stabilized while the collapsed state population progressively disappears, and a significant fraction of the population is found in the hairpin state. Urea, therefore, exhibits a typical denaturing effect. In strong contrast with TMAO and in agreement with a previous study,<sup>30</sup> we show in Figure S1 of the Supporting Information that urea readily denatures hydrophobic polymers (e.g.,  $\epsilon_b = 0.4$  kJ/mol), yet its denaturing effect becomes more prominent as  $\epsilon_b$  increases.

To assess the robustness of our results, we also repeated our simulations with an  $\epsilon_b$  of 1.0 kJ/mol using a different water model<sup>39</sup> and found very similar results (see the text and Figure S3 of the Supporting Information). Although the force field we have employed for TMAO has been widely employed in the past and clearly behaves as a protective osmolyte,<sup>24,25,29</sup> it has recently been criticized because it underestimates the osmotic pressure at high solute concentrations.<sup>27</sup> We have repeated our simulations at 1 M using the modified ("osmotic") version of the force field of Garcia et al.<sup>27</sup> As shown in Figure S2 of the Supporting Information, its effect on the polymer chain nonetheless differs very little from what we observed using the aforementioned force field.

Our simulations show that TMAO acts as a protective osmolyte and urea as a denaturant on the polymer chain for an  $\epsilon_b$  of 1.0 kJ/mol. TMAO thus acts on this chain like it acts on many proteins as found experimentally,<sup>6</sup> showing that its effect extends to purely uncharged polymer chains of moderate hydrophobicity. TMAO's ability to act as a protecting osmolyte depends on the properties of the polymer on which it is acting as shown by its sensitivity to the value of the polymer bead  $\epsilon_b$ . TMAO seems to have little effect on strongly hydrophobic chains. Urea, on the other hand, still denatures them. In the following, we aim to better understand the effect of both osmolytes on the polymer chain with an  $\epsilon_b$  of 1.0 kJ/mol.

**Molecular Mechanism of Osmolyte-Induced (Un)-folding.** *Interpretation Based on Preferential Binding and Chemical Potential of Osmolytes.* It has been suggested in the literature that denaturants exhibit preferential interaction with protein surfaces while protective osmolytes are preferentially excluded from the surface<sup>4–8</sup> because of unfavorable interactions.<sup>6,8</sup> Therefore, such behavior should be observed in both local bulk partition coefficient  $K_p$  (eq 1) and preferential binding coefficient  $\Gamma$  (eq 2).

In panels A and B of Figure 4, we compare the dependence of  $K_p$  on polymer conformation as a function of the distance from the polymer in both TMAO and urea solutions. If the local domain is defined as the polymer's first solvation shell, then the representative values for  $K_p$  (and later  $\Gamma$ ) should be taken to be near  $\approx 6$  Å (dashed line), which corresponds to the first minima of the radial distribution functions between the polymer and cosolvent molecules (urea or TMAO). As expected, urea molecules accumulate next to both collapsed and extended states of the polymer, leading to a  $K_p$  of  $>1$  (Figure 4B).  $K_p$  is only slightly sensitive to the polymer conformation but is always slightly higher in the extended state. The local bulk partition coefficient of TMAO is also greater than 1 (Figure 4A), implying that TMAO also binds to the polymer surface. This result contradicts the popular view that

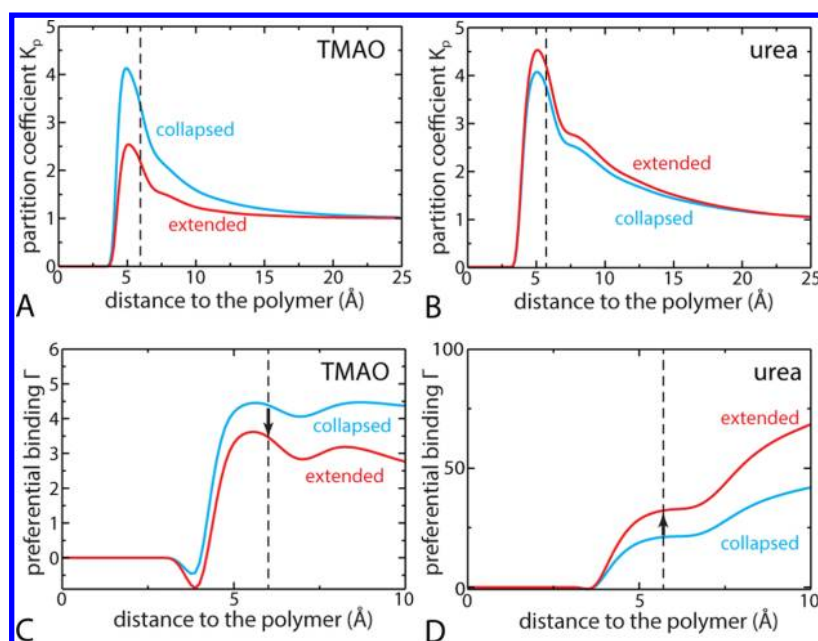


**Figure 4.** Preferential binding constants of TMAO in 1 M TMAO (red) and urea in 7 M urea (green) as a function of the distance to the polymer (for chains with an  $\epsilon_b$  of 1.0 kJ/mol), frozen in a collapsed (black) or extended (red) configuration. Vertical dashed lines indicate the positions of the polymer first solvation shell in each case (6 Å for TMAO and 5.7 Å for urea), and the black arrows in panels C and D represent the relevant value of  $\Delta\Gamma$ .

protective osmolytes are believed to be preferentially excluded from the protein surface.<sup>4–8</sup> However, this should not be surprising because TMAO is mostly hydrophobic and thus might be better accommodated in the polymer hydration shell than in bulk solution, but a key observation is that  $K_p$  displays significant conformation dependence: it is higher near a collapsed configuration than near an extended configuration. Therefore, TMAO strongly interacts with the polymer ( $K_p > 1$ ), but there is an effective depletion next to extended conformations of the polymer relative to collapsed conformations.

Although the local bulk partition coefficient provides a better description of the preferential interaction because of its intensive nature, it is not directly connected to experimental observables. In contrast, the preferential binding coefficient  $\Gamma$  can be measured experimentally, e.g., using the vapor-pressure osmometry technique.<sup>7</sup> The effect of preferential binding on a conformational equilibrium between the folded and unfolded configurations [ $F \rightleftharpoons U$  (with an equilibrium constant  $K$ )] is usually understood in terms of the thermodynamic calculation first introduced by Wyman and Tanford,<sup>2,3</sup> which leads to

$$\frac{\partial \ln K}{\partial \ln a_s} = \Delta\Gamma_{F \rightarrow U} \quad (4)$$

where  $a_s$  is the activity of the cosolvent in the binary solution. According to eq 4, an increase in the concentration of the cosolvent would lead to the biomolecule unfolding if  $\Delta\Gamma > 0$  and in contrast would favor the folded state over the unfolded one if  $\Delta\Gamma < 0$ .

In panels C and D of Figure 4, we show the average preferential binding coefficients ( $\Gamma$ ) for both collapsed and extended conformations in TMAO and urea solutions. As already discussed above, one should consider the  $\Gamma$  values at the distance corresponding to the polymer first solvation shell. Not surprisingly, in all cases,  $\Gamma$  is positive, which is equivalent to a  $K_p$  of  $>1$  (Figure 4A,B). Similarly, the trends in the

difference between the extended and collapsed configurations ( $\Delta\Gamma$ ) follow that of  $\Delta K_p$ :  $\Delta\Gamma$  is negative for TMAO, which stabilizes the folded state over the unfolded one, while the positive  $\Delta\Gamma$  for urea clearly corresponds to its denaturing effect. Our results are therefore in agreement with the current consensus about the osmolyte effect<sup>4–8</sup> summarized by eq 4.

The main difference between our work and previous studies of proteins is that the sign of  $\Delta\Gamma$  is different from that of  $\Gamma$  for TMAO (they have the same sign for urea). This surprising observation can be understood if we consider the relationship between  $K_p$  and  $\Gamma$ . Indeed, combining eqs 1 and 2 with the hypothesis that the bulk domain is large with respect to the local domain (i.e.,  $\langle n_x \rangle \ll N_x^{\text{tot}}$ ) leads to

$$\Gamma = \langle n_s \rangle \left( 1 - \frac{1}{K_p} \right) \quad (5)$$

Therefore,  $\Delta\Gamma$  will depend on both  $\Delta\langle n_s \rangle$  and  $\Delta(1/K_p)$  (note that these two terms are not independent of each other). In experimental studies of proteins, it was found that  $\Gamma$  is proportional to the solvent surface accessible area  $S$ .<sup>7</sup> Because  $\langle n_s \rangle$  is also proportional to  $S$ ,  $K_p$  is expected to be the same regardless of whether the protein is folded. This may not be surprising given that the nature of the exposed groups is the same in the folded and unfolded states. However, for our polymer,  $K_p$  is very much conformation-dependent, while  $n_s$  is only marginally higher in the extended state. This therefore provides an explanation for why  $\Delta\Gamma$  is negative while TMAO always accumulates in the hydration shell ( $\Gamma > 0$ ). Finally, it is interesting to note that simulations of decaalanine have found  $\Gamma$  to be positive for TMAO<sup>29</sup> even though it was observed to behave as a protective osmolyte.

**Conformation Dependence of the Osmolyte Chemical Potentials in the Polymer First Solvation Shell.** To obtain a better understanding of how TMAO can preferentially bind to the polymer surface yet still behave as a protective osmolyte

**Table 1. Different Free Energy Contributions (in kilocalories per mole) for Inserting Single Osmolyte Molecules in the First Solvation Shell of the Polymer ( $\epsilon_b = 1.0$  kJ/mol) in 1 M TMAO and 7 M Urea and  $\Delta\mu^{\text{bulk}}$  and  $N_k$  Values<sup>a</sup>**

system	$G_{\text{vdw}}$	$G_{\text{coulomb}}$	$G_{\text{total}}$	$\Delta\mu^{\text{bulk}}$	$\langle N_k \rangle$
TMAO					
bulk	+1.99(0.02)	-13.97(0.02)	-11.97(0.01)	0	-
collapsed	-0.52(0.36)	-13.08(0.22)	-13.60(0.27)	-1.63	6.2(0.2)
extended	+1.04(0.45)	-13.80(0.08)	-12.76(0.38)	-0.79	6.3(0.6)
urea					
bulk	-0.17(0.04)	-13.27(0.05)	-13.44(0.09)	0	-
collapsed	-1.33(0.71)	-12.45(0.53)	-13.78(0.20)	-0.33	28.6(0.3)
extended	-0.99(0.29)	-12.91(0.23)	-13.90(0.15)	-0.46	41.9(0.8)

<sup>a</sup>  $\Delta\mu^{\text{bulk}}$  represents the difference with respect to the bulk solution, and the average number of molecules in first solvation shell of the polymer ( $N_k$ ) is also given. Standard deviations are given in parentheses.

favoring the polymer collapsed state, we investigate the free energy changes (chemical potential) associated with the insertion of a single osmolyte or water molecule next to different conformations (both collapsed and extended) of the polymer. These chemical potentials were determined from thermodynamic integration (see Simulation Model and Methods and the text and Figures S4 and S5 of the Supporting Information). Insertion of a TMAO and a water molecule in the 1 M TMAO solution (or urea and water in the 7 M urea solution) was considered in three different cases: in the bulk, i.e., far from the polymer; in the first hydration shell of the polymer frozen in a collapsed configuration; and in the first hydration shell of the polymer frozen in an extended configuration.

Table 1 lists the results of thermodynamic integration, namely, the van der Waals and electrostatic contributions to the chemical potentials of urea and TMAO in the different cases. In all cases, insertion of an osmolyte molecule is more favorable next to the polymer than it is in the bulk: this is in agreement with the preferential binding values discussed above. However, the chemical potentials of TMAO and urea, relative to bulk values, follow opposite trends as far as conformation dependence is concerned. An inserted single TMAO molecule is more stable (has a lower free energy) next to the collapsed conformation of the polymer than next to the extended conformation. Its free energy is lower by 0.8 kcal/mol per TMAO molecule. This is mainly due to the more favorable free energy contribution from the van der Waals interaction, which overcomes the slight destabilization in the electrostatic contribution in the collapsed conformation because of less exposure to water or other TMAO molecules in the collapsed state than in the extended state. Given the importance of the van der Waals term for this (mostly) hydrophobic molecule, the total free energy change is dominated by this contribution. In urea, however, the van der Waals term is small and does not totally compensate for the electrostatic contribution. Therefore, the insertion of a urea molecule is more favorable next to the extended state.

The observed differences and respective contributions of van der Waals and electrostatic free energy, which drive the preferential interaction with one state or another, suggest a mostly enthalpic origin to this behavior. This is confirmed by considering the distributions of both van der Waals and electrostatic energy distributions for a single osmolyte molecule in the hydration shell of the polymer, either in a collapsed or in an extended conformation (see the text and Table S1 of the Supporting Information). The observed trends are similar to that found from the FEP study: TMAO interacts preferentially

with the polymer collapsed state because of the van der Waals contribution, leading to a difference of  $\approx 0.2$  kcal/mol as compared to the extended state and difference of  $\approx 0.5$  kcal/mol with respect to the bulk phase. In contrast, a slight stabilization of urea in the extended polymer hydration shell with respect to the collapsed state is found ( $\approx 0.2$  kcal/mol) and appears to be driven by the electrostatic contribution. In both conformations, a significant stabilization is found as compared to the bulk phase ( $\approx 1.5$  kcal/mol).

*A Free Energy-Based Model for the Action of a Protecting and Denaturing Osmolyte.* The discussion in the previous paragraphs has focused on only the contributions of the chemical potential of the osmolyte (TMAO or urea) to the free energy difference between the polymer collapsed and extended states. We now try to build a free energy-based thermodynamic model based on the FEP data given above, with the goal of validating it against the net PMF profiles of the polymer in the respective solutions (as previously discussed in Figure 3). The net free energy change for going from a collapsed to an extended configuration can be expressed as

$$\begin{aligned}
 \Delta G^{\text{C-E}} &= \Delta G_{\text{gas}}^{\text{C-E}} + \sum \Delta G_k^{\text{C-E}} \\
 &= \Delta G_{\text{gas}}^{\text{C-E}} + \Delta G_W^{\text{C-E}} + \Delta G_{\text{CS}}^{\text{C-E}} \\
 &= \Delta G_{\text{gas}}^{\text{C-E}} + [N_w^{\text{E}} \mu_w^{\text{E}} - N_w^{\text{C}} \mu_w^{\text{C}}] \\
 &\quad + [N_s^{\text{E}} \mu_s^{\text{E}} - N_s^{\text{C}} \mu_s^{\text{C}}]
 \end{aligned}
 \tag{6}$$

where  $N_k^{\text{C}}$  ( $N_k^{\text{E}}$ ) is the average number of solvent molecules of type  $k$  (water  $w$  or osmolyte  $s$ ) in the first hydration shell of the polymer in a collapsed (extended) configuration and  $\mu_k^{\text{C}}$  ( $\mu_k^{\text{E}}$ ) is the associated chemical potential. We assume here that the chemical potentials of molecules beyond the first hydration shell are similar for both polymer configurations.

To evaluate eq 6, we must separately determine three individual contributions.

(a) The first term of the equation corresponds to the free energy difference between the collapsed and extended states of the polymer itself in the gas phase. It was obtained by repeating our simulations in the gas phase and by performing umbrella sampling calculations to estimate the free energy difference between the collapsed and extended states in the absence of solvent ( $\Delta G_{\text{gas}}^{\text{C-E}}$ ), which was found to be 9.6 kcal/mol in favor of the collapsed conformation.

(b) To calculate the second term, which describes water's contribution to the total free energy difference, we repeated our FEP calculations for water as well using the same method as

**Table 2.** Total Free Energy Costs [ $\Delta\mu^{\text{bulk}}$  (with respect to the bulk solution reference)] for Inserting Single Water Molecules into the First Solvation Shell of the Polymer ( $\epsilon_b = 1.0$  kJ/mol) in Pure Water, 1 M TMAO, and 7 M urea (in kilocalories per mole) and Average Numbers of Water Molecules in the Polymer First Hydration Shell ( $\langle N_k \rangle$ )<sup>a</sup>

system	$\Delta\mu^{\text{bulk}}$	$\langle N_k \rangle$
pure water		
collapsed	-0.17(0.04)	73.8
extended	-0.15(0.02)	111.3
TMAO		
collapsed	-0.08(0.05)	66.9
extended	-0.11(0.04)	106.6
urea		
collapsed	-0.13(0.14)	33.0
extended	-0.17(0.31)	43.5

<sup>a</sup>Standard deviations are given in parentheses.

detailed above for the osmolyte molecules. Results are listed in Table 2. In all cases (bulk, TMAO, or urea solutions), the difference in chemical potential between inserting a water molecule next to the collapsed or next to the extended state is very small, and slightly negative with respect to bulk. At the same time, the hydration number is significantly increasing because of a larger surface area in the extended state. Both the changes in chemical potential ( $\delta\mu_w = \mu_w^E - \mu_w^C$ ) and that of the number of molecules ( $\delta N_w = N_w^E - N_w^C$ ) contribute to the total free energy difference between the collapsed and extended states due to water molecules. A detailed analysis discussed in the text and Table S2 of the Supporting Information shows that, in all cases, the dominant contributions logically arise from  $\delta N_w$ .

(c) The third term describes the contribution of osmolyte molecules (TMAO or urea) to the net free energy difference. The chemical potentials in each configuration were already discussed and are listed in Table 1, which also contains the total number of osmolyte molecules in the polymer first hydration shell. As for water, we can define  $\delta\mu_s = \mu_s^E - \mu_s^C$  and  $\delta N_s = N_s^E - N_s^C$ . For urea, both  $\delta\mu_s$  and  $\delta N_s$  make a negative contribution to the solvent-induced free energy difference, which therefore favors the extended state. For TMAO, the two terms bring opposite contributions (text and Table S2 of the Supporting Information). While a positive  $\delta N_s$  favors the extended conformation, it is the dominant contribution of the large  $\delta\mu_s$  that leads to a positive  $\Delta G_s^{C-E}$ , stabilizing the collapsed state relative to the extended one.

Figure 5 represents these three different individual contributions schematically. In pure water, the water contribution favors the extended state, as shown above. However, it does not totally compensate for the polymer contribution (this will depend on the value of  $\epsilon$ ), so that the folded state is still the most stable in this case, as calculated independently with our umbrella sampling simulations (Figure 3). In the TMAO solution, the water contribution is only slightly perturbed with respect to the pure water case, but TMAO molecules will bring a contribution favoring the collapsed state, in agreement with our earlier estimation based on PMF calculations (Figure 3). Finally, in the urea solution, the urea contribution stabilizes the extended conformation greatly so that the overall free energy difference becomes favorable toward extended conformations, as we have observed.

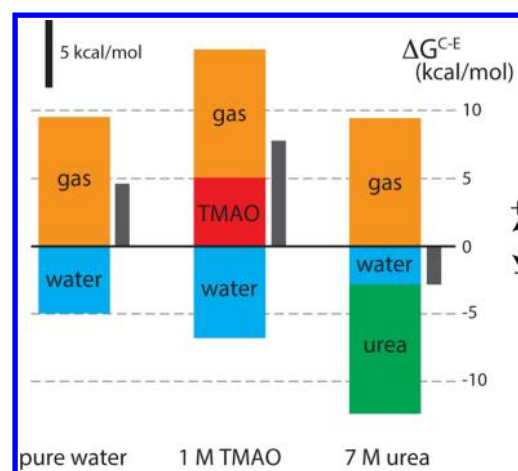


**Figure 5.** Histograms showing the different contributions to the free energy cost of inserting water or osmolyte molecules into the polymer hydration shell.

The semiquantitative agreement that is observed in all three cases with the free energy differences calculated from umbrella sampling simulations further validates this approach. Note, however, that for TMAO and urea solutions, we systematically overestimate the respective stabilization. A possible explanation for this discrepancy is that we consider only a few sites for insertion of an osmolyte or a water molecule in the hydration shell; another source of discrepancy could arise from neglecting the contribution of molecules in the second solvation shell. However, the fact that the trend is correctly and self-consistently predicted and also that the energy distributions exhibit exactly the same behavior makes us confident in this approach. Finally, the decomposition presented in the text of the Supporting Information in terms of the respective contributions of  $\delta\mu_s$  and  $\delta N_s$  also suggests that an osmolyte's behavior cannot be predicted from the sign of  $\delta\mu_s$  alone, as detailed in the text of the Supporting Information.<sup>a</sup>

#### IV. CONCLUSIONS

In this paper, we considered the effect of osmolytes (TMAO and urea) on a simple polymer, consisting of a short LJ chain similar to an alkane or lipid chain in aqueous solutions of the two osmolytes. This model is reminiscent of the model used in our previous paper<sup>30</sup> directed at understanding urea denaturation of hydrophobic collapse.

Here we determined the free energy landscapes of the hydrophobic polymer as a function of its radius of gyration. We show that 1 M TMAO and 7 M urea act dramatically differently on model polymer chains and their behaviors are sensitive to the strength of the attractive dispersion interactions of the chain with its environment: when these dispersion interactions are sufficiently strong, TMAO suppresses the formation of extended conformations of the hydrophobic polymer as compared to water, while urea promotes the formation of extended conformations. Quite surprisingly, we find that both protecting and denaturing osmolytes strongly interact with the polymer (with both having a preferential binding constant greater than zero), in contrast with existing explanations of the osmolyte effect. An extensive free energy analysis suggests that protective osmolytes are not necessarily excluded from the polymer surface. What really matters is the effective depletion of the osmolyte as the polymer conformation changes, in agreement with the current consensus about the osmolyte



effect.<sup>4–8</sup> Indeed, for TMAO, it is the much more favorable free energy of insertion of a single osmolyte near the collapsed configurations of the polymer than near the extended configurations that dictates its propensity to drive the system toward the collapsed conformation, and therefore to lead to its protective effect. This appears to be driven by van der Waals interactions. In contrast, urea is preferentially stabilized next to the extended conformation because the smaller van der Waals contributions do not compensate for the electrostatic contribution, suggesting this as an explanation of its denaturing effect.

A thermodynamic model taking into account the different contributions (gas phase, water, and osmolyte) to the polymer conformational equilibrium was developed. In the aqueous solution of urea, the free energy contribution coming from urea and water easily cooperates to shift the polymer toward extended conformations of the polymer. In the aqueous solution of TMAO, TMAO's free energy contribution favors the collapsed conformation, and it is able to overcome the water's free energy contribution that favors the extended conformation: overall, the equilibrium is shifted toward the collapsed conformation.

We believe that this simple thermodynamic model provides an interesting perspective for explaining the role of protecting and denaturing osmolytes on simple macromolecules. Although the model is very simple, it provides fresh insights into the action of various osmolytes. Manipulation of simple polymers at the single-molecule level has been recently achieved,<sup>40</sup> and we believe that the effect of osmolytes such as urea or TMAO on the polymer conformational equilibrium could be probed by such techniques. From a simulation perspective, it will be interesting in the future to extend our free energy-based approach to systems of increasing complexity like charged polymers, real peptides, or proteins to shed light on the role of osmolytes in macromolecular conformations.

## ■ ASSOCIATED CONTENT

### 📄 Supporting Information

Effect of bead interaction parameter  $\epsilon_b$  on the polymer conformational equilibrium in pure water and in aqueous solutions of TMAO and urea, results for an alternative TMAO force field, results for an alternative water model, details about the thermodynamics integrations, energy distribution for solute molecules in the polymer first hydration shell, and decomposition of the solvent contribution to the free energy between the polymer collapsed and extended states. This material is available free of charge via the Internet at <http://pubs.acs.org>.

## ■ AUTHOR INFORMATION

### Corresponding Author

\*E-mail: [bb8@columbia.edu](mailto:bb8@columbia.edu). Phone: (212) 854-2186.

### Notes

The authors declare no competing financial interest.

## ■ ACKNOWLEDGMENTS

This work was supported by grants from the National Institutes of Health (GM4330 to B.J.B.) and by the National Science Foundation (NSF) (Grant CHE-0910943). We gratefully acknowledge the computational support of the Computational Center for Nanotechnology Innovations (CCNI) at Rensselaer Polytechnic Institute. This work used the Extreme Science and

Engineering Discovery Environment (XSEDE), which is supported by NSF Grant OCI-1053575.

## ■ ADDITIONAL NOTE

<sup>a</sup>Indeed, the main  $\delta N_s$  contribution (which is equal to  $\mu_s^C \delta N_s$ ) can overcome that of  $\delta \mu_s$  if the relative variations of the hydration number when going from collapsed to extended conformations are larger than that of the associated chemical potentials, even if the osmolyte molecules are more stable around the collapsed conformations.

## ■ REFERENCES

- (1) Yancey, P. H.; Clark, M. E.; Hand, S. C.; Bowlus, R. D.; Somero, G. N. Living with Water Stress: Evolution of Osmolyte Systems. *Science* **1982**, *217*, 1214–1222.
- (2) Wyman, J. Linked Functions and Reciprocal Effects in Hemoglobin: A Second Look. *Adv. Protein Chem.* **1964**, *19*, 223–286.
- (3) Tanford, C. Extension of the Theory of Linked Functions to Incorporate the Effects of Protein Hydration. *J. Mol. Biol.* **1969**, *39*, 539–544.
- (4) Timasheff, S. N. Protein-Solvent Preferential Interactions, Protein Hydration, and the Modulation of Biochemical Reactions by Solvent Components. *Proc. Natl. Acad. Sci. U.S.A.* **2002**, *99*, 9721–9726.
- (5) Parsegian, V. A.; Rand, R. P.; Rau, D. C. Osmotic Stress, Crowding, Preferential Hydration, and Binding: A Comparison of Perspectives. *Proc. Natl. Acad. Sci. U.S.A.* **2000**, *97*, 3987–3992.
- (6) Bolen, D.; Rose, G. Structure and Energetics of the Hydrogen-Bonded Backbone in Protein Folding. *Annu. Rev. Biochem.* **2008**, *77*, 339–362.
- (7) Courtenay, E. S.; Capp, M. W.; Anderson, C. F.; Record, M. T., Jr. Vapor Pressure Osmometry Studies of Osmolyte-Protein Interactions: Implications for the Action of Osmoprotectants in Vivo and for the Interpretation of “Osmotic Stress” Experiments in Vitro. *Biochemistry* **2000**, *39*, 4455–4471.
- (8) Canchi, D. R.; Garcia, A. E. Cosolvent Effects on Protein Stability. *Annu. Rev. Phys. Chem.* **2013**, *64*, 273–293.
- (9) Street, T. O.; Bolen, D. W.; Rose, G. D. A Molecular Mechanism for Osmolyte-Induced Protein Stability. *Proc. Natl. Acad. Sci. U.S.A.* **2006**, *103*, 13997–14002.
- (10) Wang, A. J.; Bolen, D. W. A Naturally Occurring Protective System in Urea-Rich Cells: Mechanism of Osmolyte Protection of Proteins against Urea Denaturation. *Biochemistry* **1997**, *36*, 9101–9108.
- (11) Hochachka, P. W., and Somero, G. N. (2002) *Biochemical Adaptation. Mechanism and Process in Physiological Evolution*, Oxford University Press, New York.
- (12) Lin, T. Y.; Timasheff, S. N. Why Do Some Organisms Use a Urea-Methylamine Mixture as Osmolyte: Thermodynamic Compensation of Urea and Trimethylamine *N*-oxide Interactions with Proteins. *Biochemistry* **1994**, *33*, 12695–12701.
- (13) Tatzelt, J.; Prusiner, S.; Welch, W. Chemical Chaperones Interfere with the Formation of Scrapie Prion Protein. *EMBO J.* **1996**, *15*, 6363–6373.
- (14) Nandi, P. K.; Bera, A.; Sizaret, P.-Y. Osmolyte Trimethylamine *N*-oxide Converts Recombinant  $\alpha$ -Helical Prion Protein to its Soluble  $\beta$ -Structured Form at High Temperature. *J. Mol. Biol.* **2006**, *362*, 810–820.
- (15) Tseng, H. C.; Graves, D. J. Natural Methylamine Osmolytes, Trimethylamine *N*-oxide and Betaine, Increase Tau-Induced Polymerization of Microtubules. *Biochem. Biophys. Res. Commun.* **1998**, *250*, 726–730.
- (16) Scaramozzino, F.; Peterson, D. W.; Farmer, P.; Gerig, J. T.; Graves, D. J.; Lew, J. TMAO promotes Fibrillization and Microtubule Assembly Activity in the C-terminal Repeat Region of Tau. *Biochemistry* **2006**, *45*, 3684–3691.
- (17) Uversky, V. N.; Li, J.; Fink, A. L. Trimethylamine *N*-oxide-Induced Folding of  $\alpha$ -Synuclein. *FEBS Lett.* **2001**, *509*, 31–35.

- (18) Morello, J. P.; Petaja-Repo, U. E.; Bichet, D. G.; Bouvier, M. Pharmacological Chaperones: A New Twist on Receptor Folding. *Trends Pharmacol. Sci.* **2000**, *21*, 466–469.
- (19) Tang, W. H. W.; Wang, Z.; Levison, B. S.; Koeth, R. A.; Britt, E. B.; Fu, X.; Wu, Y.; Hazen, S. L. Intestinal Microbial Metabolism of Phosphatidylcholine and Cardiovascular Risk. *N. Engl. J. Med.* **2013**, *368*, 1575–1584.
- (20) Bennion, B. J.; Daggett, V. Counteraction of Urea-Induced Protein Denaturation by Trimethylamine *N*-oxide: A Chemical Chaperone at Atomic Resolution. *Proc. Natl. Acad. Sci. U.S.A.* **2004**, *101*, 6433–6438.
- (21) Sharp, K. A.; Madan, B.; Manas, E.; Vanderkooi, J. M. Water Structure Changes Induced by Hydrophobic and Polar Solutes Revealed by Simulations and Infrared Spectroscopy. *J. Chem. Phys.* **2001**, *114*, 1791–1796.
- (22) Hunger, J.; Tielrooij, K.-J.; Buchner, R.; Bonn, M.; Bakker, H. J. Complex Formation in Aqueous Trimethylamine *N*-oxide (TMAO) Solutions. *J. Phys. Chem. B* **2012**, *116*, 4783–4795.
- (23) Athawale, M. V.; Dordick, J. S.; Garde, S. Osmolyte Trimethylamine *N*-oxide Does Not Affect the Strength of Hydrophobic Interactions: Origin of Osmolyte Compatibility. *Biophys. J.* **2005**, *89*, 858–866.
- (24) Cho, S. S.; Reddy, G.; Straub, J. E.; Thirumalai, D. Entropic Stabilization of Proteins by TMAO. *J. Phys. Chem. B* **2011**, *115*, 13401–13407.
- (25) Hu, C. Y.; Lynch, G. C.; Kokubo, H.; Pettitt, B. M. Trimethylamine *N*-oxide Influence on the Backbone of Proteins: An Oligoglycine Model. *Proteins* **2010**, *78*, 695–704.
- (26) Stirnemann, G.; Hynes, J. T.; Laage, D. Water Hydrogen Bond Dynamics in Aqueous Solutions of Amphiphiles. *J. Phys. Chem. B* **2010**, *114*, 3052–3059.
- (27) Canchi, D. R.; Jayasimha, P.; Rau, D. C.; Makhatazde, G. I.; Garcia, A. E. Molecular Mechanism for the Preferential Exclusion of TMAO from Protein Surfaces. *J. Phys. Chem. B* **2012**, *116*, 12095–12104.
- (28) Paul, S.; Patey, G. N. The Influence of Urea and Trimethylamine *N*-oxide on Hydrophobic Interactions. *J. Phys. Chem. B* **2007**, *111*, 7932–7933.
- (29) Kokubo, H.; Hu, C.; Pettitt, B. M. Peptide Conformational Preferences in Osmolyte Solutions: Transfer Free Energies of Decaalanine Folding. *J. Am. Chem. Soc.* **2011**, *133*, 1849–1858.
- (30) Zangi, R.; Zhou, R.; Berne, B. J. Urea's Action on Hydrophobic Interactions. *J. Am. Chem. Soc.* **2009**, *131*, 1535–1541.
- (31) Berendsen, H. J. C.; Grigera, J. R.; Straatsma, T. P. The Missing Term in Effective Pair Potentials. *J. Phys. Chem.* **1987**, *91*, 6269–6271.
- (32) Duffy, E. M.; Severance, D.; Jorgensen, W. L. Urea: Potential Functions, log *P*, and Free Energy of Hydration. *Isr. J. Chem.* **1993**, *33*, 323–330.
- (33) Kast, K. M.; Brickman, J.; Kast, S. M.; Berry, R. S. Binary Phases of Aliphatic *N*-Oxides and Water: Force Field Development and Molecular Dynamics Simulation. *J. Phys. Chem. A* **2003**, *107*, 5342–5351.
- (34) Hess, B.; Kutzner, C.; Van der Spoel, D.; Lindahl, E. GROMACS 4: Algorithms for Highly Efficient, Load-Balanced, and Scalable Molecular Simulation. *J. Chem. Theory Comput.* **2008**, *4*, 435–447.
- (35) Bonomi, M.; Branduardi, D.; Bussi, G.; Camilloni, C.; Parrinello, M. PLUMED: A Portable Plugin for Free-Energy Calculations with Molecular Dynamics. *Comput. Phys. Commun.* **2009**, *180*, 1961–1972.
- (36) Kumar, S.; Bouzida, D.; Swendsen, R. H.; Kollman, P. A.; Rosenberg, J. M. The Weighted Histogram Analysis Method for Free-Energy Calculations on Biomolecules. I. The Method. *J. Comput. Chem.* **1992**, *13*, 1011–1021.
- (37) Grossfield, A. WHAM: The Weighted Histogram Analysis Method, version 2.0 (<http://membrane.urmc.rochester.edu/content/wham>).
- (38) Shukla, D.; Shinde, C.; Trout, B. L. Molecular Computations of Preferential Interaction Coefficients of Proteins. *J. Phys. Chem. B* **2009**, *113*, 12546–12554.
- (39) Jorgensen, W.; Chandrasekhar, J.; Madura, J.; Impey, R.; Klein, M. Comparison of Simple Potential Functions for Simulating Liquid Water. *J. Chem. Phys.* **1983**, *79*, 926–935.
- (40) Li, I. T. S.; Walker, G. C. Signature of Hydrophobic Hydration in a Single Polymer. *Proc. Natl. Acad. Sci. U.S.A.* **2011**, *108*, 16527–16532.